Cell Reports, Volume *43*

Supplemental information

AMPK regulates Bcl2-L-13-mediated mitophagy induction for cardioprotection

Tomokazu Murakawa, Jumpei Ito, Mara-Camelia Rusu, Manabu Taneike, Shigemiki Omiya, Javier Moncayo-Arlandi, Chiaki Nakanishi, Ryuta Sugihara, Hiroki Nishida, Kentaro Mine, Roland Fleck, Min Zhang, Kazuhiko Nishida, Ajay M. Shah, Osamu Yamaguchi, Yasushi Sakata, and Kinya Otsu

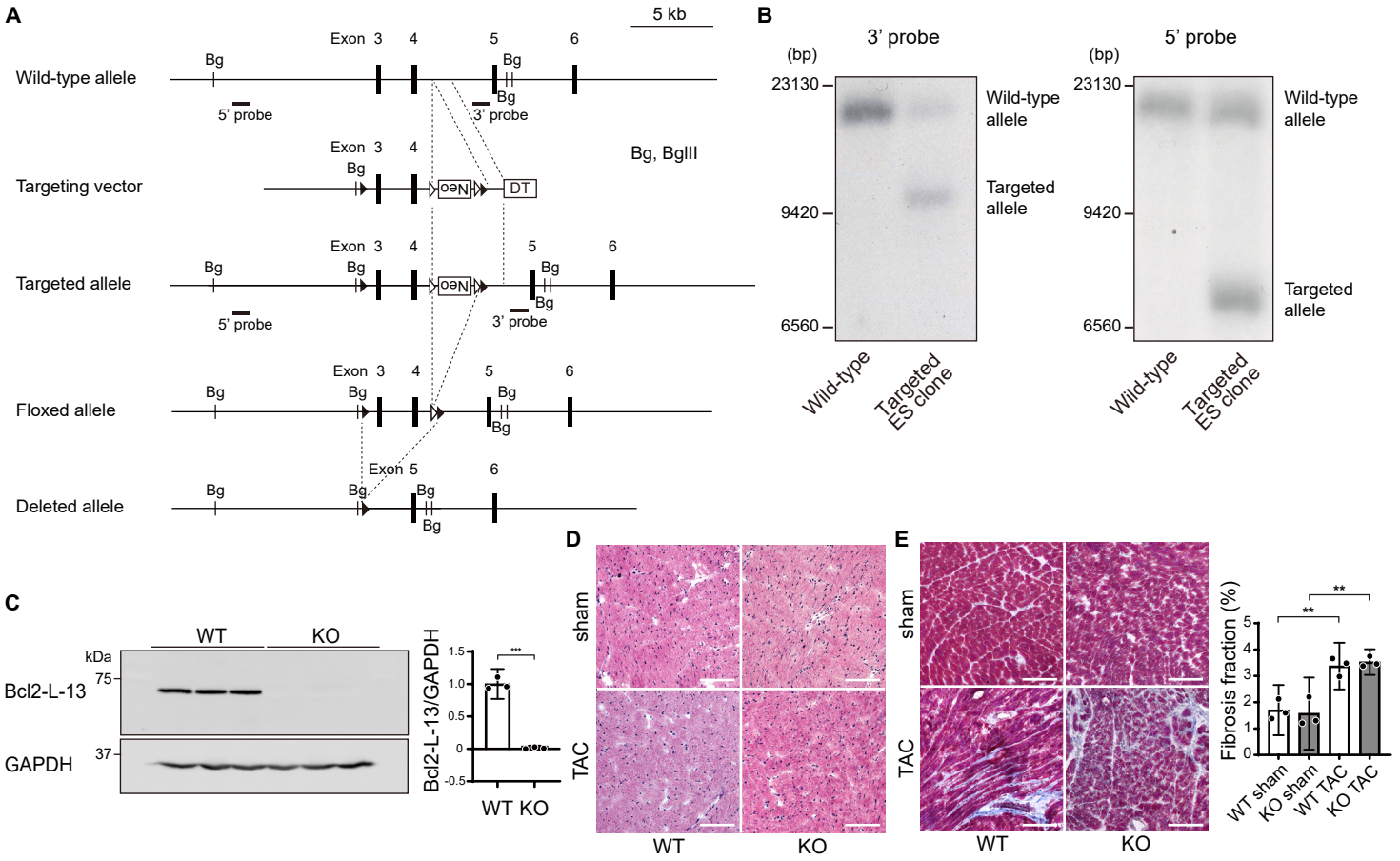

Figure S1. Targeted modification of the *Bcl2l13* gene, and histological analyses of *Bcl2l13*$^{-/-}$ mice four weeks after TAC, related to Figure 1

(A) Schematic structures of genomic *Bcl2l13* sequences, targeting vector, targeted allele, floxed allele, and *Bcl2l13*$^{-/-}$ (deleted) allele (from top to bottom). The black and white arrowheads represent *loxP* and flippase recognition target sites, respectively. The targeting construct includes the PGK-neo cassette (*Neo*) flanked by flippase recognition target sites and a diphtheria toxin (*DT*) gene. The bar-labeled probe corresponds to the sequence used for Southern blotting analysis in (B). Bg, BglII restriction site.

(B) Genomic analysis of ES cells. Genomic DNA was isolated from ES cells, digested with BglII, and analyzed via Southern blotting with 3' and 5' probes.

(C) Protein expression levels of Bcl2-L-13 in *Bcl2l13*$^{+/+}$ (WT) and *Bcl2l13*$^{-/-}$ (KO) hearts. Left ventricular homogenates from *Bcl2l13*$^{+/+}$ and *Bcl2l13*$^{-/-}$ mice were analyzed by Western blotting. The bar graph shows densitometric analysis. The average value for WT mice was set to 1 (n = 3).

(D) Hematoxylin-eosin-stained heart sections. Scale bar, 100 μm.

(E) Masson's trichrome-stained heart sections. Scale bar, 100 μm. Quantitative analysis of fibrosis fraction is shown in the bar graph (n = 3).

Results are shown as mean with 95% CI. Statistical analysis by unpaired, two-tailed t-test in (C) and a one-way ANOVA followed by Tukey–Kramer's *post hoc* test in (E). All pairwise comparisons were performed in Tukey–Kramer's *post hoc* test. $^{**}P < 0.01$, $^{***}P < 0.001$.

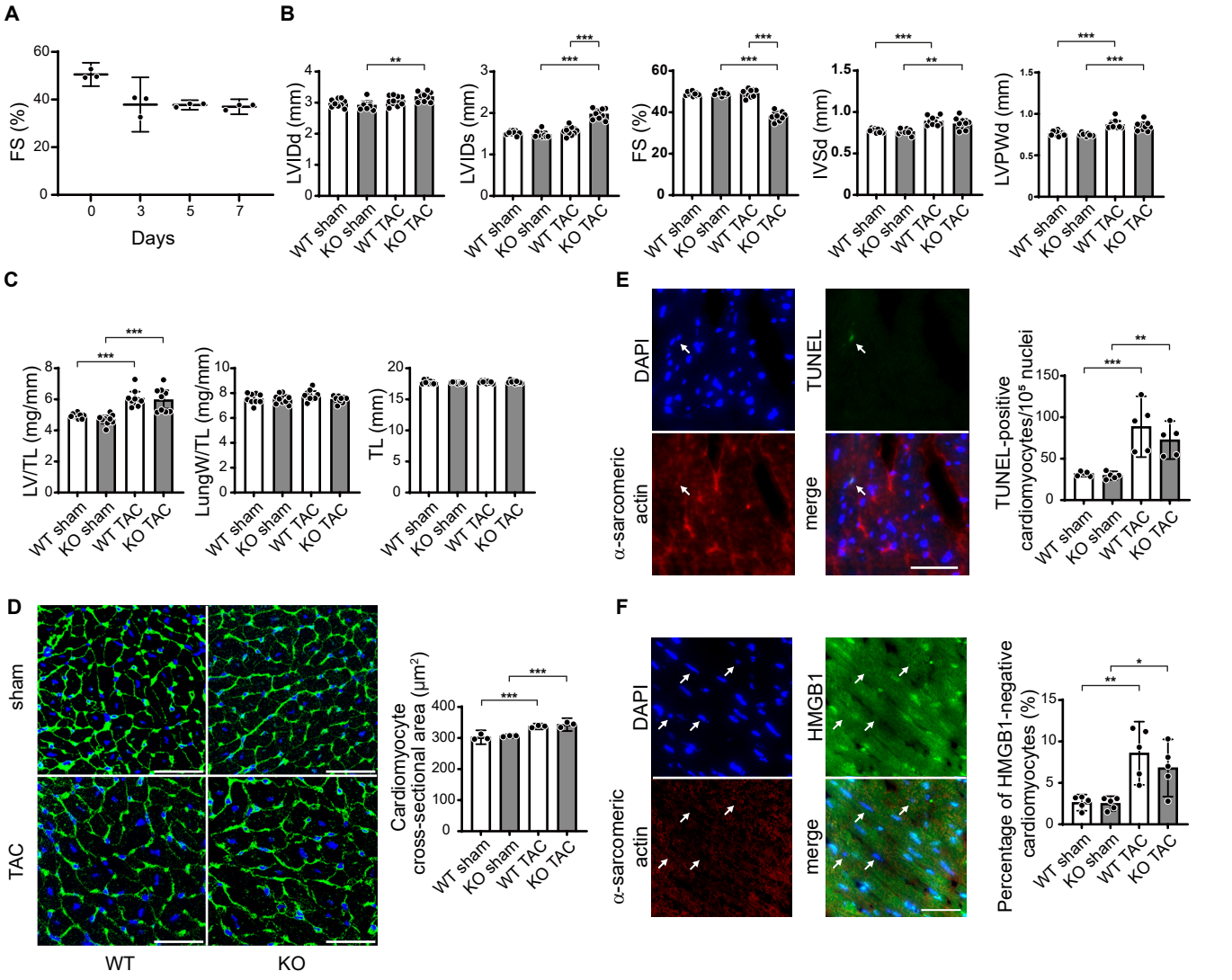

Figure S2. Analyses of *Bcl2l13*$^{-/-}$ mice five days after TAC, related to Figure 2.
(A) Analysis of fractional shortening after TAC operation in *Bcl2l13*$^{-/-}$ mice. Each data point represents the mean with 95% CI of 3 independent biological replicates.
(B and C) Echocardiographic parameters are shown in (B), and physiological parameters are shown in (C). $n = 10$.
(D) Wheat germ agglutinin-stained heart sections. Scale bar, 50 μm. Cardiomyocyte cross-sectional areas were measured by tracing the outline of 100 myocytes in the non-fibrotic area of each section ($n = 3$).
(E) Representative images of TUNEL-staining (green) in the heart sections. Arrows indicate a TUNEL-positive nucleus. Scale bar, 50 μm. Red, α-sarcomeric actin; blue, DAPI. The right graph shows a quantitative analysis of TUNEL-positive cardiomyocytes. ($n = 5$).
(F) Immunofluorescence analysis of HMGB1 (green) in the heart after TAC ($n = 5$). Arrows indicate HMGB1-negative nuclei. Scale bar, 50 μm. Red, α-sarcomeric actin; blue, DAPI. The right graph shows the percentage of HMGB1-negative cardiomyocytes.
Results are shown as mean with 95% CI. Statistical analysis by one-way ANOVA followed by Tukey–Kramer's *post hoc* test. All pairwise comparisons were performed. *$P < 0.05$, **$P < 0.01$, ***$P < 0.001$.

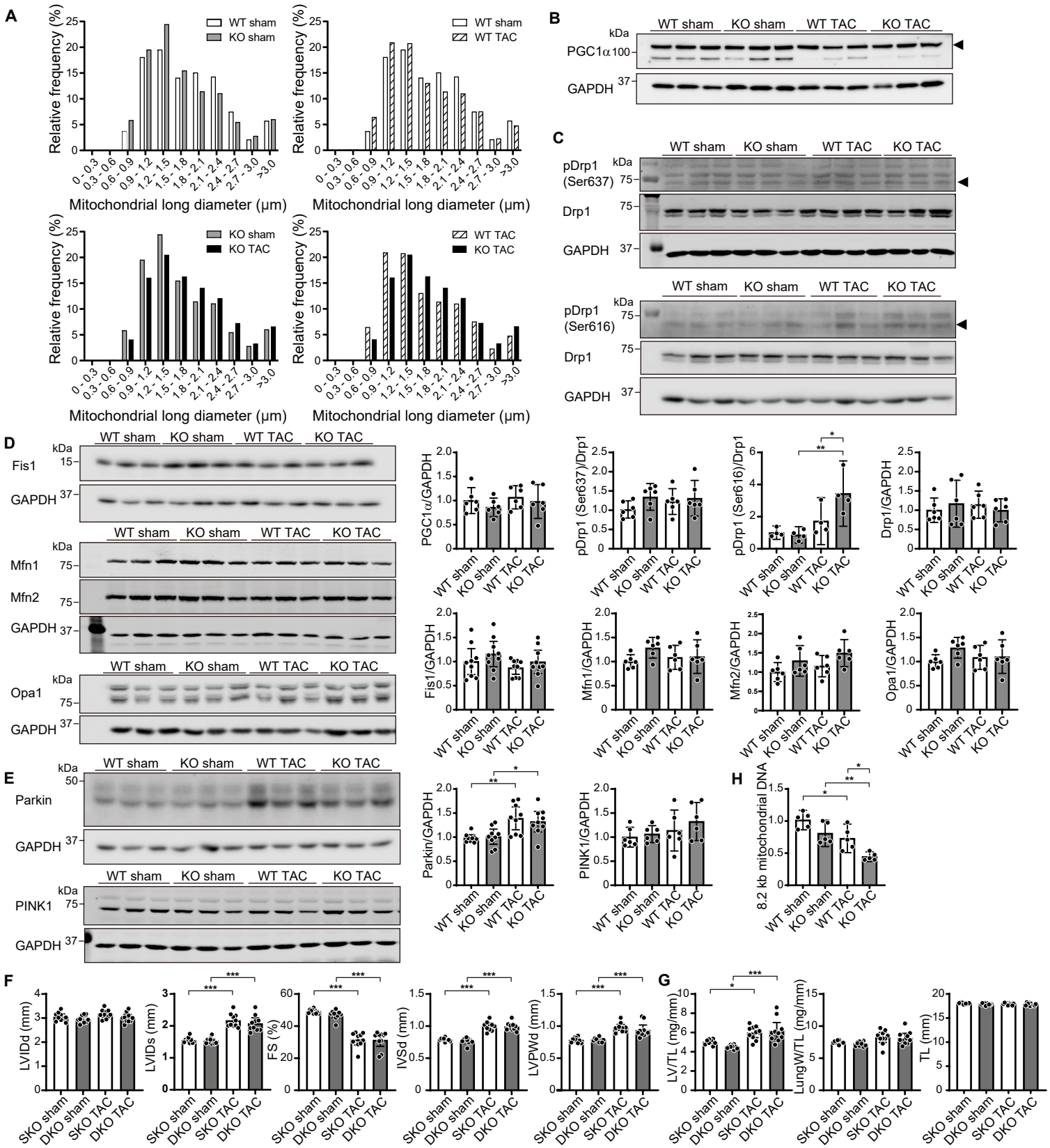

Figure S3. Ultrastructural and biochemical analyses of *Bcl2l13*$^{-/-}$ mice five days after TAC and echocardiographic and physiological analyses of *Bcl2l13*$^{-/-}$*Prk2*$^{-/-}$ mice, related to Figure 2.

(A) A histogram visualizing the distribution of the long diameter of mitochondria measured in Figure 2B.

(B-E) Heart extracts were immunoblotted with the indicated antibodies (n = 4 - 9). Densitometric analysis is shown in the bar graphs. The average value for the WT sham group was set to 1.

(F and G) *Bcl2l13*$^{-/-}$*Prk2*$^{+/+}$ (SKO) and *Bcl2l13*$^{-/-}$*Prk2*$^{-/-}$ (DKO) mice were subjected to TAC. The mice were analyzed four weeks after the TAC operation (n = 10). Echocardiographic parameters are shown in (F), and physiological parameters are shown in (G).

(H) mitochondrial DNA (mtDNA) damage was assessed by measurement of the level of replicated 8.2 kb mtDNA using mouse Real-time PCR Mitochondrial DNA Damage Analysis Kit. The damage to the mtDNA results in the inhibition of PCR of 8.2 kb mtDNA. The average value for the WT sham group was set to 1. n = 5.

Results are shown as mean with 95% CI. Statistical analysis by one-way ANOVA followed by Tukey–Kramer's *post hoc* test. All pairwise comparisons were performed. *P< 0.05, **P < 0.01, ***P < 0.001.

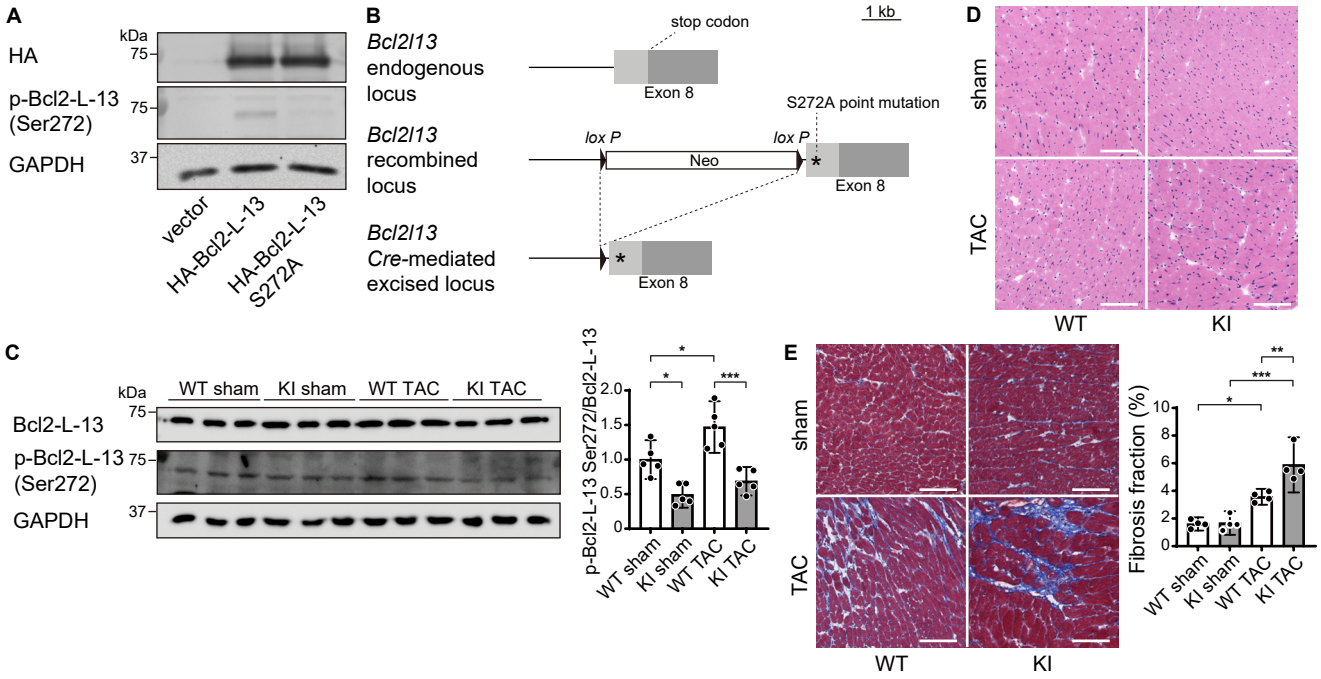

Figure S4. Histological and protein analyses in Bcl2-L-13 (S272A) knock-in mice four weeks after TAC, related to Figure 4

(A) Validation of the anti-phosho-Bcl2-L-13 (Ser272) antibody. Lysates from HEK293A cells transfected with empty vector, HA-Bcl2-L-13 or HA-Bcl2-L-13 (S272A) were subjected to immunoblotting.

(B) Schematic representation of the selected targeting strategy. Hatched rectangles represent Bcl2l13 coding sequences, grey rectangles indicate non-coding exon portions, black arrowheads indicate *loxP* sites, and asterisk indicate the inserted mutation.

(C) Heart extracts from *Bcl2L13*$^{WT/WT}$ (WT) or *Bcl2L13*$^{S272A/S272A}$ (KI) mice were immunoblotted with the indicated antibodies. Densitometric analysis is shown in the bar graph. The average value in the WT sham group was set to 1. $n = 5$.

(D) Hematoxylin-eosin-stained heart sections. Scale bar, 100 μm.

(E) Masson's trichrome-stained heart sections. Scale bar, 100 μm. Quantitative analysis of fibrosis fraction is shown in the bar graph ($n = 4$).

Results are shown as mean with 95% CI. Statistical analysis by one-way ANOVA followed by Tukey–Kramer's *post hoc* test. All pairwise comparisons were performed. **P*< 0.05, ***P* < 0.01, ****P* < 0.001.

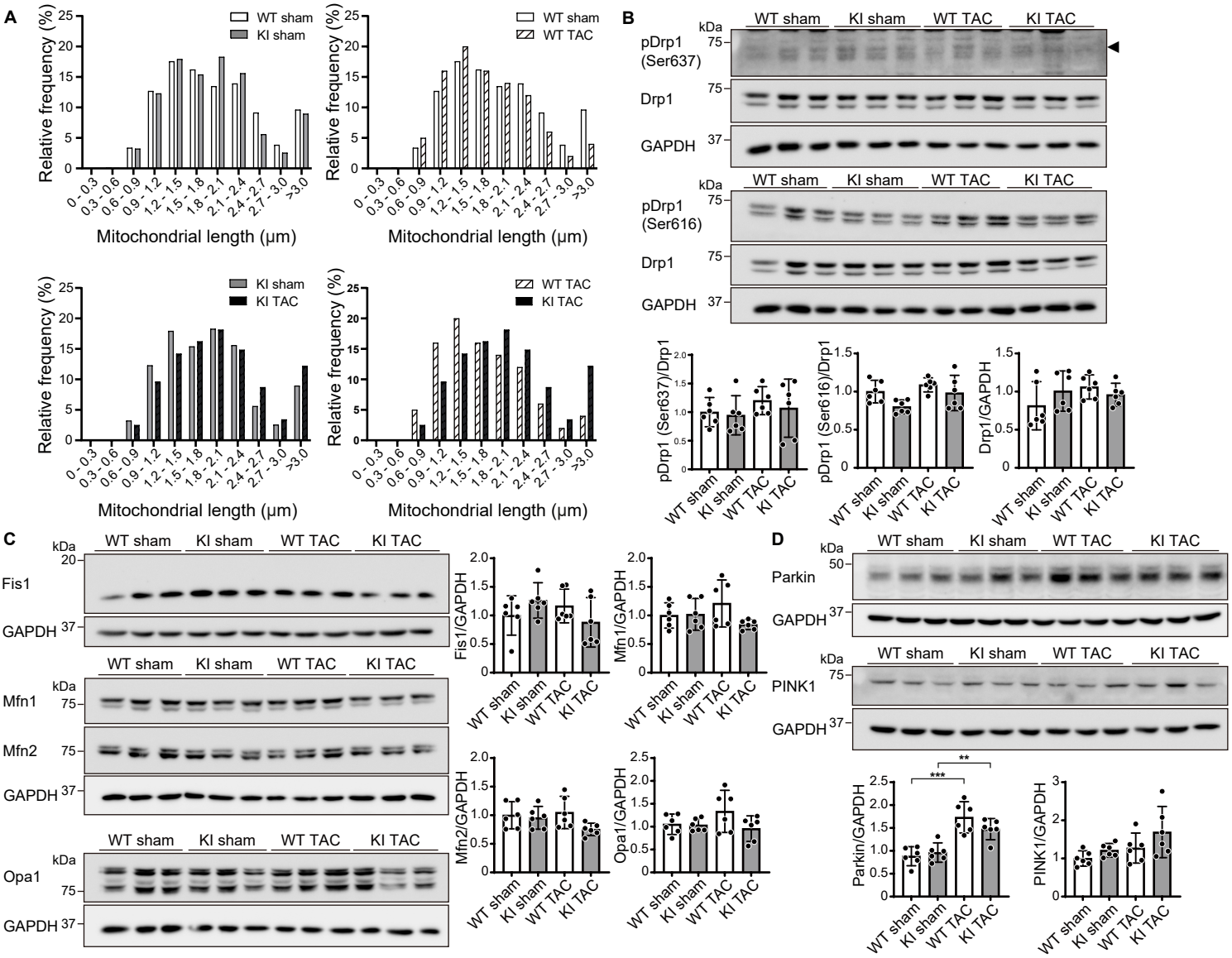

Figure S5. Ultrastructural and protein analyses in Bcl2-L-13 (S272A) knock-in mice five days after TAC, related to Figure 5

(A) A histogram visualizing the distribution of the long diameter of mitochondria measured in Figure 5A.

(B-D) Heart extracts were immunoblotted with the indicated antibodies. Densitometric analysis is shown in the bar graphs. The average value in the WT sham group was set to 1. $n = 6$.

Results are shown as mean with 95% CI. Statistical analysis by one-way ANOVA followed by Tukey–Kramer's *post hoc* test. All pairwise comparisons were performed. *$P < 0.05$, ***$P < 0.001$.

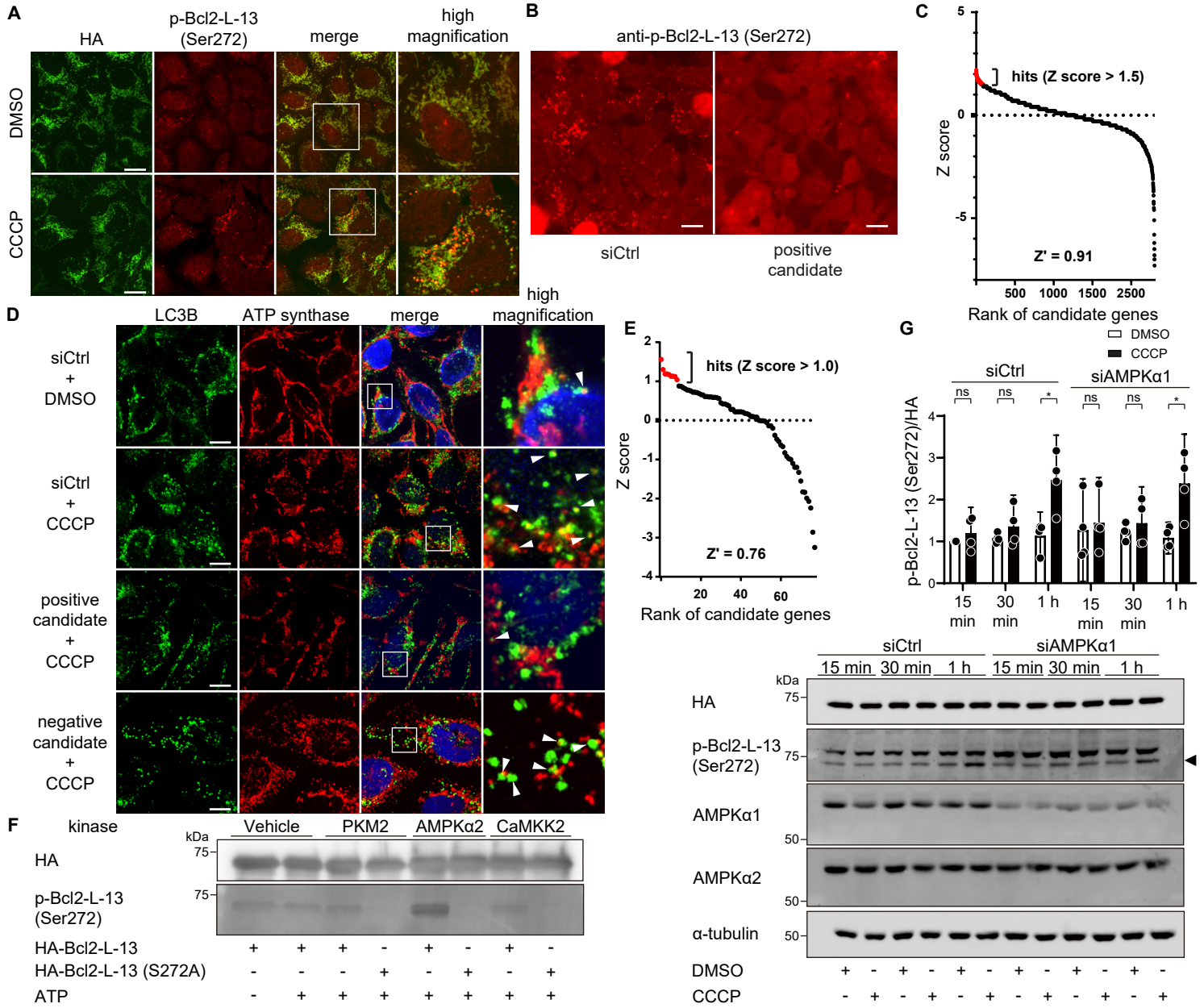

Figure S6. Screening of the responsible kinase of Bcl2-L-13 at Ser272, related to Figure 6

(A) HEK293A cells stably expressing HA-Bcl2-L-13 were treated with 15 μM CCCP and 100 nM bafilomycin A1 for four hours. Cells were fixed and immunostained with anti-phospho-Bcl2-L-13 (Ser272) and anti-HA antibodies for confocal microscopy. The boxed area is shown at higher magnification in the right panel. Scale bar, 20 μm.

(B) Representative images acquired in the primary screening. Cells were transfected with the indicated siRNAs. Seventy-two hours after transfection, cells were treated with 15 μM CCCP and 100 nM bafilomycin A1 for four hours and immunostained with an anti-phospho-Bcl2-L-13 (Ser272) antibody for automated scanning using a fluorescence microscope. For quantification of phospho-Bcl2-L-13 (Ser272)-positive dots, local maxima were determined using the “find maxima” function of the ImageJ. Scale bar, 20 μm.

(C) The candidate genes are ranked according to their Z score in the primary screening. The hits shown in red dots were chosen based on a Z score of greater than 1.5. The Z’ factor for the primary screening was calculated using the DMSO-treated samples (positive control for inhibition) and control siRNA-treated samples (negative control for inhibition).

(D) Representative images acquired in the secondary screening. HEK293A cells were transfected with the indicated siRNAs. Seventy-two hours after transfection, cells were treated with 15 μM CCCP and 100 nM bafilomycin A1 for four hours and immunostained with anti-LC3B and anti-ATP synthase antibodies for confocal microscopy. Images in the box at higher magnification are shown in the right panels. Arrowheads indicate the puncta recognized as colocalized by the software. Scale bar, 10 μm.

(E) The candidate genes are ranked according to their Z score in the secondary screening. The hits shown in red dots were chosen based on a Z score of greater than 1.0. The Z’ factor for the secondary screening was calculated using the DMSO-treated samples and control siRNA-treated samples.

(F) *In vitro* kinase assay. Bacterial synthesized HA-Bcl2-L-13 or HA-Bcl2-L-13 (S272A) was mixed with purified candidate proteins and ATP. After 30 minutes of incubation at 37°C, the reaction mix was subjected to Western blotting using an anti-phospho-Bcl2-L-13 antibody.

(G) The effect of AMPKα1 knockdown on CCCP-induced Bcl2-L-13 phosphorylation. HEK293A cells stably expressing HA-Bcl2-L-13 were transfected with the control siRNA (siCtrl) or siAMPKα1 for 72 hours. Cells were then treated with DMSO or 15 μM CCCP for the indicated times, and cell lysates were subjected to Western blot analysis. Densitometric analysis of phospho-Bcl2-L-13 (Ser272) is shown in the bar graph. The value for the siCtrl transfection and 15-minute DMSO treatment group in each experiment was set to 1 (*n* = 4). Results are shown as mean with 95% CI. Statistical analysis by unpaired, two-tailed *t*-test. *P < 0.05. ns: not significant.

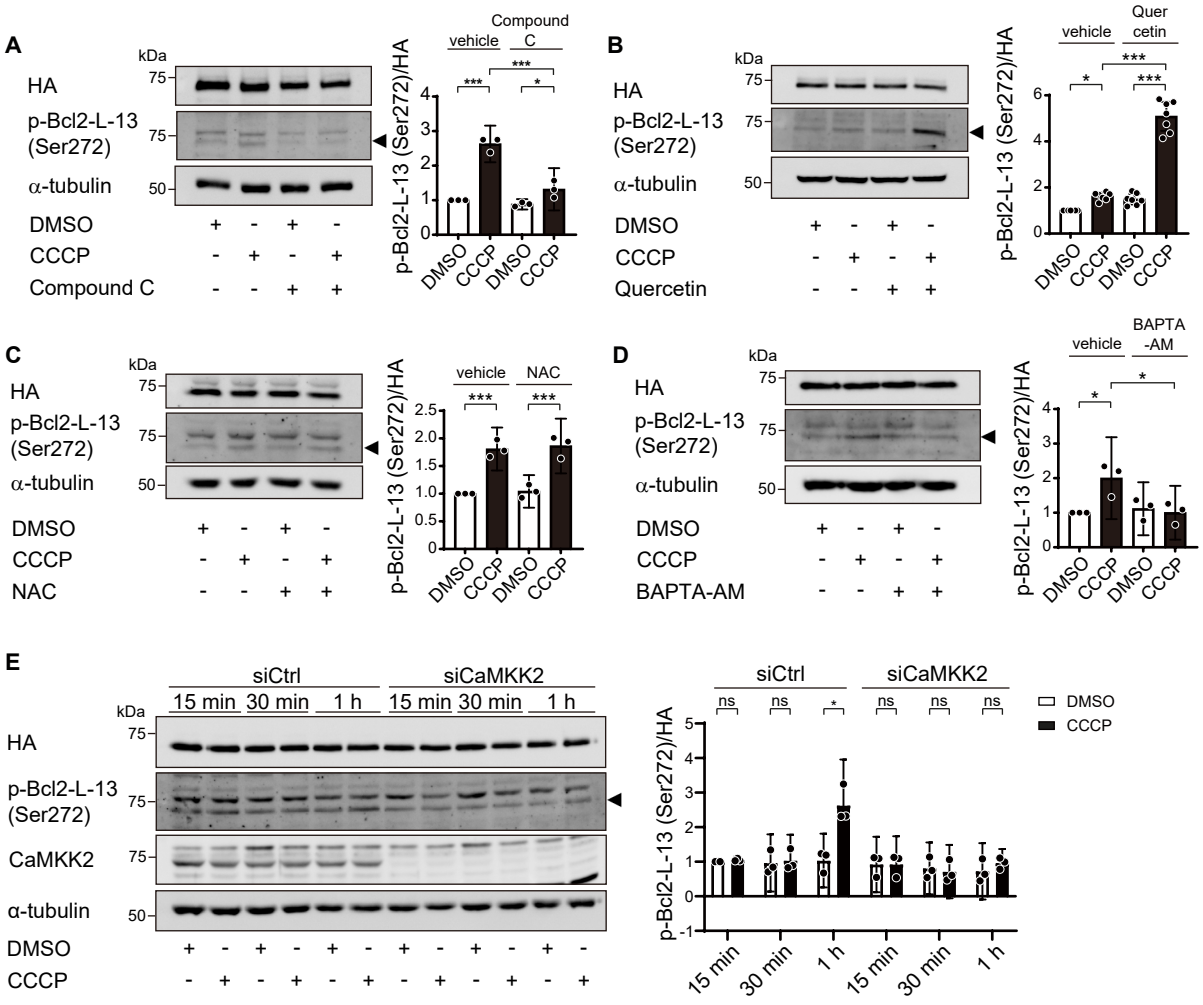

Figure S7. Regulation of the phosphorylation of Bcl2-L-13 (Ser272), related to Figure 6

(A-D) The effect of indicated drugs (10 μM Compound C, or 100 μM Quercetin, 10 μM N-Acetyl-L-cysteine (NAC), 10 μM BAPTA-AM) on CCCP-induced Bcl2-L-13 phosphorylation. HEK293A cells stably expressing HA-Bcl2-L-13 were treated with DMSO or CCCP and indicated drugs for one hour, and cell lysates were subjected to Western blot analysis. Densitometric analysis of phospho-Bcl2-L-13 (Ser272) is shown in the bar graph. The value for the DMSO and vehicle treatment group in each experiment was set to 1 (n = 3 - 7).

(E) The effect of CaMKK2 knockdown on CCCP-induced Bcl2-L-13 phosphorylation. HEK293A cells stably expressing HA-Bcl2-L-13 were transfected with the control siRNA (siCtrl) or siCaMKK2 for 72 hours. Cells were then treated with DMSO or 15 μM CCCP for the indicated times, and cell lysates were subjected to Western blot analysis. Densitometric analysis of phospho-Bcl2-L-13 (Ser272) is shown in the bar graph. The value for the siCtrl transfection and 15-minute DMSO treatment group in each experiment was set to 1 (n = 3).

Results are shown as mean with 95% CI. Statistical analysis by one-way ANOVA followed by Tukey–Kramer's *post hoc* test in (A-D) and unpaired, two-tailed *t*-tests in (E). All pairwise comparisons were performed. *P < 0.05, **P < 0.01, ***P < 0.001. ns, not significant.

Table S1. Physiological and echocardiographic parameters in 10-week-old *Bcl2l13*$^{+/+}$ and *Bcl2l13*$^{-/-}$ mice at baseline, related to Figure 1

	Bcl2l13$^{+/+}$ (*n* = 9)		*Bcl2l13*$^{-/-}$ (*n* = 8)		
	mean	**95% CI**	**mean**	**95% CI**	
Body weight (g)	**24.2**	**22.8 to 25.6**	**23.5**	**23.5 to 24.7**	***P* = 0.8700**
Blood pressure (mmHg)	**93**	**83 to 102**	**96**	**89 to 102**	***P* = 0.5393**
Heart rate (bpm)	**703**	**675 to 732**	**693**	**666 to 719**	***P* = 0.5230**
Heart weight / TL (mg/mm)	**6.7**	**6.3 to 7.1**	**6.5**	**6.1 to 6.9**	***P* = 0.4474**
Lung weight / TL (mg/mm)	**7.6**	**7.2 to 7.9**	**7.4**	**7.3 to 7.5**	***P* = 0.4604**
TL (mm)	**17.5**	**17.3 to 17.7**	**17.6**	**17.5 to 17.8**	***P* = 0.1633**
IVSd (mm)	**0.75**	**0.73 to 0.77**	**0.76**	**0.73 to 0.79**	***P* = 0.3686**
LVIDd (mm)	**2.95**	**2.84 to 3.05**	**3.01**	**2.92 to 3.10**	***P* = 0.3033**
LVIDs (mm)	**1.48**	**1.43 to 1.53**	**1.52**	**1.46 to 1.58**	***P* = 0.2405**
LVPWd (mm)	**0.74**	**0.73 to 0.75**	**0.76**	**0.74 to 0.78**	***P* = 0.1522**
FS (%)	**49.8**	**48.9 to 50.7**	**49.5**	**48.6 to 50.4**	***P* = 0.5898**

TL, tibia length; IVSd, end-diastolic interventricular septum thickness; LVIDd, end-diastolic left ventricular internal dimension; LVIDs, end-systolic left ventricular internal dimension; LVPWd, end-diastolic left ventricular posterior wall thickness; FS, fractional shortening. Paired data were evaluated by Student's *t*-test.

Table S2. Physiological and echocardiographic parameters in 10-week-old *Bcl2l13*$^{WT/WT}$ and *Bcl2l13*$^{S272A/S272A}$ mice at baseline, related to Figure 4

	Bcl2l13$^{WT/WT}$ (*n* = 8)		*Bcl2l13*$^{S272A/S272A}$ (*n* = 8)		
	mean	**95% CI**	**mean**	**95% CI**	
Body weight (g)	**25.2**	**24.3 to 26.2**	**25.7**	**24.2 to 27.1**	***P* = 0.5590**
Blood pressure (mmHg)	**97**	**86 to 107**	**102**	**94 to 110**	***P* = 0.3863**
Heart rate (bpm)	**738**	**711 to 765**	**719**	**697 to 742**	***P* = 0.2412**
Heart weight / TL (mg/mm)	**6.9**	**6.5 to 7.2**	**6.8 ± 0.2**	**6.4 to 7.2**	***P* = 0.8436**
Lung weight / TL (mg/mm)	**7.5**	**7.3 to 7.7**	**7.5**	**7.2 to 7.8**	***P* = 0.9157**
TL (mm)	**17.8**	**17.4 to 18.2**	**17.8**	**17.6 to 18.0**	***P* > 0.9999**
IVSd (mm)	**0.77**	**0.75 to 0.79**	**0.76**	**0.74 to 0.78**	***P* = 0.8506**
LVIDd (mm)	**3.04**	**2.88 to 3.19**	**2.92**	**2.73 to 3.10**	***P* = 0.2565**
LVIDs (mm)	**1.54**	**1.45 to 1.64**	**1.50**	**1.44 to 1.57**	***P* = 0.4208**
LVPWd (mm)	**0.75**	**0.74 to 0.77**	**0.76**	**0.74 to 0.77**	***P* = 0.6617**
FS (%)	**49.2**	**48.1 to 50.4**	**49.1**	**48.2 to 50.0**	***P* = 0.8546**

TL, tibia length; IVSd, end-diastolic interventricular septum thickness; LVIDd, end-diastolic left ventricular internal dimension; LVIDs, end-systolic left ventricular internal dimension; LVPWd, end-diastolic left ventricular posterior wall thickness; FS, fractional shortening. Paired data were evaluated by Student's *t*-test.

Table S3. Candidate list after the 1st screen, related to Figure 6

Gene symbol	Gene ID	Gene name
AAK1	22848	AP2-associated kinase 1
ACVR1B	91	activin A receptor, type IB
ACVR2A	92	activin A receptor, type IIA
ADCK5	203054	aarF domain containing kinase 5
ADRBK1	156	adrenergic, beta, receptor kinase 1
AK1	203	adenylate kinase 1
AK5	26289	adenylate kinase 5
AKAP7	9465	A kinase (PRKA) anchor protein 7
ANKK1	255239	ankyrin repeat and kinase domain containing 1
AURKC	6795	aurora kinase C
CAMK2A	815	calcium/calmodulin-dependent protein kinase (CaM kinase) II alpha
CAMK2N1	55450	calcium/calmodulin-dependent protein kinase I
CAMK1G	57172	calcium/calmodulin-dependent protein kinase IG
CAMKK2	10645	calcium/calmodulin-dependent protein kinase kinase 2, beta
CDC42BPA	8476	CDC42 binding protein kinase alpha (MRCK)
CERKL	375298	ceramide kinase-like
C9orf96	169436	chromosome 9 open reading frame 96
CNKSR1	10256	connector enhancer of kinase suppressor of Ras 1
CDC42BPA	8476	cyclin-dependent kinase 10
CDKL1	8814	cyclin-dependent kinase-like 1 (CDC2-related kinase)
DAPK2	23604	death-associated protein kinase 2
DCK	1633	deoxycytidine kinase
DGUOK	1716	deoxyguanosine kinase
EPHA3	2042	EPH receptor A3
FASTK	10922	Fas-activated serine/threonine kinase
FGFRL1	53834	fibroblast growth factor receptor-like 1
FRAP1	2475	FK506 binding protein 12-rapamycin associated protein 1

Table S3. Candidate list after the 1st screen (continued).

Gene symbol	Gene ID	Gene name
FLT1	2321	fms-related tyrosine kinase 1 (vascular endothelial growth factor/vascular permeability factor receptor)
FLT3	2322	fms-related tyrosine kinase 3
GALK1	2584	galactokinase 1
GSG2	83903	germ cell associated 2 (haspin)
HGS	9146	hepatocyte growth factor-regulated tyrosine kinase substrate
IPPK	64768	inositol 1,3,4,5,6-pentakisphosphate 2-kinase
IHPK3	117283	inositol hexaphosphate kinase 3
IRAK2	3656	interleukin-1 receptor-associated kinase 2
LMTK3	114783	lemur tyrosine kinase 3
LOC375133	375133	-
LOC389599	389599	-
MARK4	57787	MAP/microtubule affinity-regulating kinase 4
MAGI3	260425	membrane associated guanylate kinase, WW and PDZ domain containing 3
MAST2	23139	microtubule associated serine/threonine kinase 2
MAPK15	225689	mitogen-activated protein kinase 15
MAPK4	5596	mitogen-activated protein kinase 4 (ERK4)
MAP3K12	7786	mitogen-activated protein kinase kinase kinase 12
MAP3K7	6885	mitogen-activated protein kinase kinase kinase 7 (TAK1)
MAP4K5	11183	mitogen-activated protein kinase kinase kinase kinase 5
MLKL	197259	mixed lineage kinase domain-like
NLK	51701	nemo-like kinase
NTRK1	4914	neurotrophic tyrosine kinase, receptor, type 1
NME9	347736	NME/NM23 family member 9
NUAK1	9891	NUAK family, SNF1-like kinase, 1
PI4KB	5298	phosphatidylinositol 4-kinase, catalytic, beta
PLXNB3	5365	plexin B3
PRKCA	5578	protein kinase C, alpha

Table S3. Candidate list after the 1st screen (continued).

Gene symbol	Gene ID	Gene name
PRKAA2	5563	5'-AMP-activated protein kinase (AMPK) catalytic subunit alpha-2
PRKACB	5567	protein kinase, cAMP-dependent, catalytic, beta
PRKACG	5568	protein kinase, cAMP-dependent, catalytic, gamma
PKLR	5313	pyruvate kinase, liver and RBC
PKM2	5315	pyruvate kinase, muscle
RIPK3	11035	receptor-interacting serine-threonine kinase 3
RYK	6259	RYK receptor-like tyrosine kinase
STK10	6793	serine/threonine kinase 10
STK11	6794	serine/threonine kinase 11
STK11IP	114790	serine/threonine kinase 11 interacting protein
STK16	8576	serine/threonine kinase 16
STK32A	202374	serine/threonine kinase 32A
SGK2	10110	serum/glucocorticoid regulated kinase 2
TBK1	29110	TANK-binding kinase 1
TSSK4	283629	testis-specific serine kinase 4
TTC33	23548	tetratricopeptide repeat domain 33
TGFBR1	7046	transforming growth factor, beta receptor 1
TPR	7175	translocated promoter region (to activated MET oncogene)
TRIB3	57761	tribbles homolog 3 (Drosophila)
TYK2	7297	tyrosine kinase 2

Table S4. Candidate list after the 2nd screen, related to Figure 6

- **manual counting**

Gene symbol	Gene ID	Gene name	Kinase type
AAK1	22848	AP2-associated kinase 1	Serine/threonine-protein kinase
ACVR2A	92	activin A receptor, type IIA	Serine/threonine-protein kinase
CAMKK2	10645	calcium/calmodulin-dependent protein kinase kinase 2, beta	Serine/threonine-protein kinase
CDC42BPA	8476	CDC42 binding protein kinase alpha (MRCK)	Serine/threonine-protein kinase
CERKL	375298	ceramide kinase-like	NAD kinase
CNKSR1	10256	connector enhancer of kinase suppressor of Ras 1	MAPK activation
FASTK	10922	Fas-activated serine/threonine kinase	Serine/threonine-protein kinase
GSG2	83903	germ cell associated 2 (haspin)	Serine/threonine-protein kinase
IRAK2	3656	interleukin-1 receptor-associated kinase 2	Serine/threonine-protein kinase
MAP3K7	6885	mitogen-activated protein kinase kinase kinase 7 (TAK1)	Serine/threonine-protein kinase
MAPK4	5596	mitogen-activated protein kinase 4 (ERK4)	Serine/threonine-protein kinase
MLKL	197259	mixed lineage kinase domain-like	Pseudokinase
NLK	51701	nemo-like kinase	Serine/threonine-protein kinase
PKLR	5313	pyruvate kinase, liver and RBC	pyruvate kinase
PKM2	5315	pyruvate kinase, muscle	pyruvate kinase, Serine/threonine-protein kinase
PRKAA2	5563	5'-AMP-activated protein kinase (AMPK) catalytic subunit alpha-2	Serine/threonine-protein kinase, Tyrosine kinase
RYK	6259	RYK receptor-like tyrosine kinase	Tyrosine kinase
TRIB3	57761	tribbles homolog 3 (Drosophila)	Protein kinase inhibition

Table S4. Candidate list after the 2nd screen, related to Figure 6 (continued)

- **software counting**

Gene symbol	Gene ID	Gene name	Kinase type
MAPK4	5596	mitogen-activated protein kinase 4 (ERK4)	Serine/threonine-protein kinase
PKLR	5313	pyruvate kinase, liver and RBC	pyruvate kinase
CNKSR1	10256	connector enhancer of kinase suppressor of Ras 1	MAPK activation
GSG2	83903	germ cell associated 2 (haspin)	Serine/threonine-protein kinase
RYK	6259	RYK receptor-like tyrosine kinase	Tyrosine kinase
RIPK3	11035	receptor-interacting serine-threonine kinase 3	Serine/threonine-protein kinase
PRKACB	5567	protein kinase, cAMP-dependent, catalytic, beta	Serine/threonine-protein kinase
PRKAA2	5563	5'-AMP-activated protein kinase (AMPK) catalytic subunit alpha-2	Serine/threonine-protein kinase
PKM2	5315	pyruvate kinase, muscle	Pyruvate kinase, Serine/threonine-protein kinase